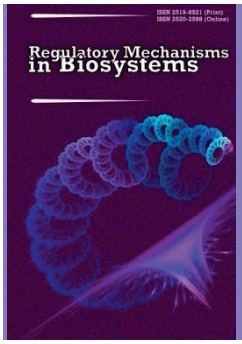

Regulatory Mechanisms in Biosystems

ISSN 2519-8521 (Print)
ISSN 2520-2588 (Online)
Regul. Mech. Biosyst.,
2024, 15(2), 327–336
doi: 10.15421/022447

In silico exploration of antinociceptive activity of 1,4-benzodiazepines: Molecular docking on α1 A-adrenoceptor, and phosphodiesterase 4

A. S. Akisheva*, V. B. Larionov**, M. Y. Golovenko**, O. A. Makarenko*, I. P. Valivodz**, I. Y. Borysiuk***, Y. O. Molodan*

**Odesa I. I. Mechnikov National University, Odesa, Ukraine*
***O. V. Bogatsky Physico-Chemical Institute of the National Academy of Sciences of Ukraine, Odesa, Ukraine*
****International Humanitarian University, Odesa, Ukraine*

Article info

Received 08.03.2024
Received in revised form 12.04.2024
Accepted 03.05.2024

Odesa I. I. Mechnikov National University, Dvoryanska st., 2, Odesa, 65082, Ukraine. Tel.: +38-050-641-86-51. E-mail: alinaakisheva@stud.onu.edu.ua

O. V. Bogatsky Physico-Chemical Institute of the National Academy of Sciences of Ukraine, Lyustdorfska Road st., 86, Odesa, 65080, Ukraine. Tel.: +38-063-508-39-89. E-mail: valivodzirina@gmail.com

International Humanitarian University, Fontanska Road, 23a, Odesa, 65016, Ukraine. Tel.: +38-067-559-51-02. E-mail: borisyuk.kaynova@gmail.com

Akisheva, A. S., Larionov, V. B., Golovenko, M. Y., Makarenko, O. A., Valivodz, I. P., Borysiuk, I. Y., & Molodan, Y. O. (2024). In silico exploration of antinociceptive activity of 1,4-benzodiazepines: Molecular docking on α1 A-adrenoceptor, and phosphodiesterase 4. Regulatory Mechanisms in Biosystems, 15(2), 327–336. doi:10.15421/022447

Recently, scientists have established that several benzodiazepines were found to enhance the activation of a cAMP response element pathway by α1A-adrenergic receptors, but this effect was attributed to off-target inhibition of phosphodiesterases 4. The study explores the pain-relief potential of 1,4-benzodiazepines using in silico methods, focusing on their interaction with α1A-adrenoceptors (α1-AR) and phosphodiesterase 4 (PDE4). AutoDock Vina-1.2.5 and Glide (Schrödinger Suite) (2023-2) were used to calculate the binding affinities and determine the features of their interactions by the molecular docking method; PlayMolecule software was used to perform molecular dynamics. Propoxazepam exhibits moderate free binding energy for α1A-adrenoceptors, as indicated by its average molecular mechanics/generalized Born surface area (MMGBSA) and Glide Score values. Compared to propoxazepam, 3-hydroxypropoxazepam has enhanced predicted affinity values for the alpha 1A adrenergic receptor, primarily due to the hydroxyl group, which facilitates the formation of additional hydrogen bonds. Propoxazepam, along with its metabolite 3-hydroxypropoxazepam, demonstrates promising interactions with PDE4A, characterized by notably low predicted free binding energy MMGBSA and strong binding affinity computed via AutoDock Vina. Among other ligands, propoxazepam demonstrates the lowest MMGBSA value with PDE4A (phosphodiesterase 4A). The best predicted binding scores of interaction with phosphodiesterase 4 is observed for propoxazepam with PDE4B (phosphodiesterase 4B) -10.3 kcal/mol, according to AutoDock Vina. Propoxazepam and its derivative 3-hydroxypropoxazepam interact with the active sites of PDE4B and PDE4D (phosphodiesterase 4 B) via a "hydrophobic clamp", a typical binding mode for PDE inhibitors, which relies on crucial hydrophobic interactions. Binding of propoxazepam and its metabolite 3-hydroxypropoxazepa to PDE4B reduces the fluctuations of M-pocket residues and supports the conclusion that ligand binding stabilizes the protein structure of PDE4B. The MMGBSA method predicts that propoxazepam and 3-hydroxypropoxazepam have the most favourable predicted binding energies with PDE4D (2FMO). Since 1,4-benzodiazepines bind to phosphodiesterase 4 similarly to its inhibitors, this may support the hypothesis that benzodiazepines may affect α1-AR by inhibiting PDE4. The study of the binding mechanisms of 1,4-benzodiazepines with phosphodiesterase 4 and alpha-1A adrenoceptors helps to expand the understanding of the analgesic and anti-inflammatory effect of benzodiazepines associated with these proteins, which can be taken into account in the development of new analgesic and anti-inflammatory agents.

Keywords: propoxazepam; docking analysis; molecular dynamic; α1-adrenergic receptors; PDE4; pain; inflammation.

Introduction

27.5 percent of the population worldwide is reported to suffer from chronic pain, which is a widespread phenomenon (Clifford, 2020; Golovenko et al., 2023). To combat the growing prevalence of chronic pain states and opioid dependency, it is crucial to comprehend the intricacies of how the body regulates pain. This issue in public health is growing, yet there are only limited therapeutic resources available to combat it. Many components are involved in the highly complex, multi-level biological system that processes pain neurologically (Milligan et al., 2019; Kachkovska et al., 2023; Tsyndrenko & Romaniuk, 2024). The development of novel analgesics with novel mechanisms of action is obstructed by numerous challenges, such as a limited understanding of the biological processes that cause pain and analgesia, and poor translation from animals to humans (Barakat et al., 2024).

"Propoxazepam", an innovative drug created by scientists of the O. V. Bogatsky Physico-Chemical Institute of the National Academy of Sciences of Ukraine and SLC "Interchim", has an original pharmacodynamic profile, and can inhibit both acute and chronic pain, as well as have anti-inflammatory and anticonvulsant effects. Propoxazepam's analgesic effect is mediated by its dopaminergic system, NMDA receptors, and alpha-1 adrenoceptors (Voloshchuk et al., 2017; Golovenko, 2021).

Midazolam, diazepam, and lorazepam, which are benzodiazepines, have been proposed to act as positive allosteric modulators (PAMs) for α1-adrenergic receptors. Multiple benzodiazepines had a positive impact on phenylephrine's stimulation of a cAMP response element pathway through α1A-and α1B-ARs; from the literature it appears that this was caused by off-target inhibition of phosphodiesterase, which are known targets of diazepam (Williams et al., 2019).

The α1-adrenergic receptors are G-protein coupled receptors that regulate neurotransmission, which bind and activate both the neurotransmitter norepinephrine and the neurohormone epinephrine. The subtypes of alpha-1-adrenergic receptors, which are known as (α1A, α1B, α1D), play different roles in neurotransmission and cognition (Perez, 2020).

The PDE4 gene family represents the most extensive amount of cAMP-specific phosphodiesterases (PDEs) and holds significant importance in regulating the dynamics and spatial-temporal aspects of cAMP signalling across various tissues and cell types (Baillie et al., 2019; Paes et al., 2022). Alternative splicing of four genes, PDE4A, PDE4B, PDE4C, and PDE4D (on chromosomes 19p13.2, 1p31, 19p13.11, and 5q12), results in the generation of at least 20–25 protein variants. PDE4 expression is ubiquitous. PDE4A is expressed relatively highly in the human brain, and the tissue distribution is specific to variants. The heart and small intestine also express PDE4A. Immune cells highly express PDE4, especially PDE4B and PDE4D isoforms (Azevedo et al., 2014). The ability of diazepam to inhibit phosphodiesterase (PDE) (especially PDE4), a known target of some benzodiazepines, was found to mediate the stimulation of a cAMP response element (CRE) reporter by activation of alpha1-ARs (Williams et al., 2019). It is probable that PDE4 inhibition can reduce neuropathic pain by moderating the expression of Cx43 in the spinal dorsal horn, given the importance of Cx43 in regulating cAMP signaling (Xu et al., 2017; Zhang et al., 2022). Additionally, PDE4B and PDE4D play a role in regulating neutrophil function, making them significant targets for pharmaceutical research aiming to develop new inhibitors for anti-inflammatory medications (Chu et al., 2021; Jin et al., 2023). The therapeutic effects of PDE4 inhibitors stem from their capacity to dampen the action of numerous natural inflammation mediators like TNF-α, IL-10, and IL-12. They also hinder the expression and increase of cell adhesion molecules involved in immune responses (Jin et al., 2023).

Recent years have seen the importance of molecular docking in *in-silico* drug development grow. This method is used to predict how a small molecule interacts with a protein at the atomic level. For molecular docking techniques, several commercial and free computational tools and algorithms are available (Agu et al., 2023). AutoDock Vina, Glide and AutoDock Gold were identified as the best docking analysis programs (Ghode & Jain, 2018; Potluri et al., 2021; Agu et al., 2023).

In order to gain a dynamic insight into biological targets and ligand binding, it has always been necessary to use complementary tools. MD, an *in silico* method, can make use of structural data obtained experimentally to estimate the possible conformations of molecular systems and the various pathways between them. The overall stability of the complex is monitored by measuring other values, including root-mean-square deviations (RMSD) from a reference configuration and atom-positional root-mean-square fluctuations (RMSF). Other methods like linear interaction energy (LIE) and using both molecular mechanics (MM) calculations along with continuum solvation models such as Poisson–Boltzmann surface area (PBSA) and generalized Born surface area (GBSA) are available. MM/GBSA methods enable the direct calculation of the binding free energy (ΔGbind) (Mortier et al., 2015). The aim of the study was the analysis of molecular interactions of the group of benzodiazepines with the alpha-1A-adrenergic receptor and phosphodiesterase 4 by molecular docking, molecular dynamic and analysis of components of these interactions.

Materials and methods

Molecular docking study. The molecular docking procedure was carried out using 3 Cryo-EM structures of α 1A- adrenergic receptor from protein data bank (www.rcsb.org): 7YM8, 7YMH, 8THL. Norepinephrine (7YMH), epinephrine (8THL), oxymetazoline (7YM8), propoxazepam, its metabolite 3-hydroxypropoxazepam, oxazepam, and diazepam were docked during the alpha1AAR research. The molecular docking procedure was executed with the use of 6 crystal structures of phosphodiesterase 4 (PDE4) from protein data bank (www.rcsb.org): 2 PDE4A (3I8V, 3TVX), 2 PDE4B (4KP6, 3W5E), 2 PDE4D (6IM6, 2FM0). The reference ligands 0MO (3I8V), pentoxifylline PNX (3TVX), 1S1 (4KP6), NVW (3W5E), AH3 (6IM6), M98 (2FM0) and benzodiazepine ligands including propoxazepam, its possible metabolite 3-hydroxypropoxazepam, oxazepam and diazepam were docked while investigating PDEs 4. Molecular docking studies of the compounds under investigation were performed with Schrödinger and AutoDock Vina-1.2.5 (http://vina.scripps.edu) and the results were compared (Trott & Olson, 2010).

Protein preparation was performed using AutoDock tools1.5.7 for docking with the AutoDock Vina-1.2.5 program. The structures of the ligands (diazepam, oxazepam, propoxazepam, 3-hydroxypropoxazepam, given in *.pdb format)) have been optimized by the value of the internal energy in the Avogadro program (v 1.2.0) and the Merck molecular force field algorithm (MMFF94).

For docking with the Schrödinger Maestro-2023-2, Protein Preparation from Schrödinger Suite was utilized for modelling the protein; the protein structure was prepared by adding hydrogen atoms, optimizing hydrogen bonds. The LigPrep module in the Schrödinger suite was used to prepare the ligands before docking. Reference ligand location was used for automated binding site detection. Ranking was given to the ligands based on their G-scores using the following formulae G-score = 0.05*vdW + 0.15*Coul + Lipo + Hbond + Metal + Rewards + RotB + Site (1), where Van der Waals energy (vdW), Coulomb energy (Coul), Lipophilic term (Lipo), Hydrogen-bonding term (Hbond), Metal-binding term (Metal), favorable hydrophobic interactions (Rewards), penalty for freezing rotatable bonds (RotB), and polar interactions in the active site (Site). The binding free energies MM-GBSA of the complexes were calculated using the Prime module in the Schrödinger suite. The formula for calculating binding energy is: DG bind = E_complex(minimized) - E_ligand(minimized) -E_receptor(minimized) (2) (Friesner et al., 2006; Halgren, 2009; Yang et al., 2021). The experimental binding free energy, was calculated as ΔG = RTln (Ki) (3). Ki values were taken from the ChEMBL database (www.ebi.ac.uk/chembl).

Molecular dynamics study. PlayMolecule software (playmolecule.com) was used to perform the ligand-protein complex simulations after starting with the output model from the docking experiments. Docking complexes obtained with AutoDock Vina were used for the molecular dynamic study (Martínez-Rosell et al., 2017). By utilizing the GAFF2 force field and the parametrization function, a ligand was created (Gianoncelli et al., 2020). The ProteinPrepare and SystemBuilder modules were used to build the complexes for simulation, using pH = 7.4, the AMBER force field, and the default experimental parameters (Cogh et al., 2021). The default settings were utilized by SimpleRun to execute a 10-ns, 12-ns simulation. The result contained the root mean square deviation (RMSD) for every frame in time and the root mean square fluctuation (RMSF) of the protein. Compared with traditional experiments, *in silico* molecular modelling can reveal the atomic details of how drugs interact with receptors, providing guidance for the rational design of receptor modulators (Beihong et al., 2018). Current investigation of ligands of alpha-1 adrenergic receptors and phosphodiesterase 4 is primarily provided using the same binding site as the reference ligand.

Results

Alpha-1 adrenergic receptor. The reference compounds have the lowest binding energies with the α1A adrenergic receptor from the MMGBSA results obtained. Among the investigated benzodiazepines, diazepam shows the lowest MMGBSA values for all receptors - 7YM8 (-56.9 kcal/mol), 7YMH (-35.7 kcal/mol), 8THL (-28.3 kcal/mol). Diazepam also has the lowest predicted Glide score of all proteins examined 7YM8 (-8.5 kcal/mol), 7YMH (-7.9 kcal/mol), 8THL (-8.1 kcal/mol), reflecting a stable ligand-receptor complex (Table 1). Based on the results from AutoDock Vina, interactions of benzodiazepines with the α1A adrenergic receptor generally show stronger binding affinities compared to those of the reference ligands.

The highest MMGBSA and Glide Score values are found in propoxazepam among all ligands (Table 1). Table 2 summarizes the binding free energies obtained from the MM-GBSA calculations in comparison with the corresponding experimental binding free energies for the α1A adrenergic receptor with reference substances.

Phosphodiesterase 4. Propoxazepam demonstrate the low value of MMGBSA for PDE4A (3I8V -55.1 kcal/mol, 3TVX -60.7 kcal/mol) and predicted docking values calculated by Vina (3I8V -8.7 kcal/mol, 3TVX -9.2 kcal/mol) (Table 3). Its metabolite 3-hydroxypropoxazepam also shows significant affinities with all subtypes of PDE4, ranging from -8.3 to -9.8 kcal/mol (AutoDock Vina).

3I8V: Diazepam and oxazepam as the reference ligand 0MO create a pi-pi stacking interaction with PHE 584. Propoxazepam and 3-hydroxypropoxazepam have a hydrophobic interaction with this residue. Diaze-

pam and 0MO also form a pi-pi stacking interaction with TYR 371. 3-hydroxypropoxazepam has a similar interaction with the reference ligand 0MO in the binding pocket, both forming water-bridged hydrogen bonds with MET 485 and HIS 372. Diazepam and 3-hydroxypropoxazepam share a halogen bond with GLN 581.

Table 1

Docking results of the studied ligands with α 1A-adrenergic receptor using AutoDock 4 and Schrödinger Maestro Glide software

Substances	7ym8 (Oxymetazoline)			7ymh (Norepinephrine)			8thl (L-epinephrine)		
	Glide Score	MMGBSA	Auto Dock Vina	Glide Score	MMGBSA	Auto Dock Vina	Glide Score	MMGBSA	Auto Dock Vina
Reference ligand	–7.5	–83.9	–8.8	–7.9	–45.6	–6.0	–7.9	–57.6	–6.0
Norepinephrine	–8.0	–52.9	–6.8	–7.9	–45.7	–6.0	–8.1	–47.7	–5.8
Epinephrine	–7.0	–60.0	–6.9	–7.9	–53.2	–6.2	–7.9	–57.7	–6.0
Propoxazepam	–6.8	–38.5	–8.7	–6.2	–17.2	–6.6	–6.0	–6.9	–5.1
3-hydroxypropoxazepam	–7.5	–47.7	–8.9	–6.9	–39.8	–5.9	–7.4	–21.0	–7.9
Oxazepam	–7.7	–39.2	–8.8	–7.3	–31.5	–7.9	–6.7	–7.1	–6.8
Diazepam	–8.5	–56.9	–9.2	–7.9	–35.7	–6.6	–8.1	–28.3	–8.3

Notes: 7ym8-Cryo-EM structure of Nb29-alpha1AAR-miniGsq complex bound to oxymetazoline, 7ymh-Cryo-EM structure of Nb29-alpha1AAR-miniGsq complex bound to noradrenaline, 8thl-Cryo-EM structure of epinephrine-bound alpha-1A-adrenergic receptor in complex with heterotrimeric Gq-protein, Glide Score – an empirical scoring function that approximates the ligand binding free energy, AutoDock Vina – binding affinity scores, calculated by open-source program for doing molecular docking AutoDock Vina, MMGBSA – Molecular Mechanics/Generalized Born Surface Area.

Table 2

Experimental binding free energies

References ligands	Ki, nM	ΔGexp, kcal/mol	MMGBSA, kcal/mol
Oxymetazoline CHEMBL1909085	16	–12.07	–83.89
Norepinephrine CHEMBL679	3000	–8.24	–52.94
Epinephrine CHEMBL679	2800	–7.71	–60.00

Notes: Ki (nM) – inhibition constant, ΔGexp – experimental binding free energy, MMGBSA – Molecular Mechanics/Generalized Born Surface Area.

3TVX: Propoxazepam and 3-hydroxypropoxazepam form a hydrogen bond with the residue ASP 530 through the hydrogen of the amide group. Propoxazepam has one more hydrogen bond with ASN 533 by oxygen of the alkoxy group. Most of the ligands (propoxazepam, diazepam, oxazepam and reference ligand 0MO) establish pi-pi stacking interaction with PHE 584. 3-hydroxypropoxazepam creates the metal coordination bond with Mg^{+2} through Oxygen of the amide group. This type of interaction is also appropriate for 0MO (by Oxygen of carbonyl group). 3-hydroxypropoxazepam forms a hydrogen bond with HIE 416 by hydroxyl group.

Table 3

Docking results (kcal/mol) of studied ligands with PDE receptor using AutoDock Vina and Schrödinger Maestro Glide software

Protein	Methods of calculation	Propoxazepam	Diazepam	Oxazepam	3-hydroxypropoxazepam	Reference ligands
3I8V (PDE4A)	AutoDock Vina	–8.7	–8.1	–8.7	–8.7	–7.3
	Glide GScore	–7.8	–8.1	–8.2	–6.1	–8.9
	MMGBSA	–55.1	–35.05	–37.9	–10.4	–24.1
3TVX (PDE4A)	AutoDock Vina	–9.2	–7.8	–8.7	–9.3	–7.2
	Glide GScore	–7.7	–8.5	–7.4	–6.7	–6.2
	MMGBSA	–60.7	–67.0	–64.6	–35.8	–68.9
4KP6 (PDE4B)	AutoDock Vina	–9.5	–9.0	–9.4	–9.8	–8.2
	Glide GScore	–6.5	–6.7	–6.0	–5.4	–6.9
	MMGBSA	–2.4	–1.4	–24.0	–29.1	1.3
3W5E (PDE4B)	AutoDock Vina	–10.3	–9.3	–10.6	–9.3	–12.2
	Glide GScore	–7.9	–9.7	–8.6	–7.9	–13.9
	MMGBSA	–37.5	–47.5	–34.3	–47.7	–103.8
6IM6 (PDE4D)	AutoDock Vina	–8.8	–8.5	–8.5	–9.0	–7.8
	Glide GScore	–	–7.3	–7.1	–5.2	–7.3
	MMGBSA	–	–50.25	–40.73	–4.04	–59.14
2FM0 (PDE4D)	AutoDock Vina	–8.7	–8.4	–8.5	–8.3	–9.6
	Glide GScore	–8.2	–8.9	–8.3	–8.2	–11.7
	MMGBSA	–52.6	–37.8	–36.3	–43.9	20.2

Notes: see Table 1, PDE4A- Phosphodiesterase 4 A, PDE4B- Phosphodiesterase 4 B, PDE4D- Phosphodiesterase 4 D, 3I8V-Crystal structure of human PDE4a with 4-(3-butoxy-4-methoxyphenyl)methyl-2-imidazolidone, 3TVX-The structure of PDE4A with pentoxifylline at 2.84A resolution, 4KP6-Crystal structure of human phosphodiesterase 4B (PDE4B) in complex with a [1,3,5]triazine derivative, 3W5E-Crystal structure of phosphodiesterase 4B in complex with compound 31e, 6IM6-Crystal structure of PDE4D complexed with a novel inhibitor, 2FM0-Crystal structure of PDE4D in complex with L-869298, 0MO-(4R)-4-(3-butoxy-4-methoxybenzyl)imidazolidin-2-one (reference substance of 3I8V), PNX-3,7-dimethyl-1-(5-oxohexyl)-3,7-dihydro-1h-purine-2,6-dione (reference substance of 3TVX), 1s1-2-ethyl-2-{[4-(methylamino)-6-(1H-1,2,4-triazol-1-yl)-1,3,5-triazin-2-yl]amino}butanenitrile (reference substance of 4KP6), NVW-N-tert-butyl-2-{4-[(5,5-dioxido-2-phenyl-7,8-dihydro-6H-thiopyrano[3,2-d]pyrimidin-4-yl)amino]phenyl}acetamide (reference substance of 3W5E), AH3-7-ethoxy-6-methoxy-3,4-dihydroisoquinoline-2(1H)-carbaldehyde (reference substance of 6IM6), M98 -(s)-3-(2-(3-cyclopropoxy-4-(difluoromethoxy)phenyl)-2-(5-(1,1,1,3,3,3-hexafluoro-2-hydroxypropan-2-yl)thiazol-2-yl)ethy l)pyridine 1-oxide (reference substance of 2FM0).

4KP6: Only diazepam manages to form a similar hydrogen bond as reference ligand 1s1 at the 4KP6 binding site with GLN 443 through oxygen from the carbonyl group. Propoxazepam and 3-hydroxypropoxazepam form a pi-pi stacking interaction with PHE 446 as reference ligand 1s1. GLN 443 has halogen bonds with oxazepam and 3-hydroxypropoxazepam. Oxazepam shows a water-bridged hydrogen bond interaction with the same amino acid residues as 1s1, through the oxygen of the carbonyl group with ASP 392, and through the NH group of the diazepine ring with TYR 233. The reference ligand 1s1 forms these water-bridged hydrogen bonds via the N of the heterocyclic triazine with ASP 392, via the NH group of the aminobutanenitrile with ASP 392, and via TYR 233.

3W5E: According to the predicted docking results (Schrödinger Maestro), Diazepam, oxazepam and the reference ligand NVW establish a hydrogen bond with GLN 443, where diazepam forms this interaction through the nitrogen of the diazepam ring, oxazepam through the nitrogen of the diazepam ring and through the hydroxyl group and NVW through the nitrogen of the pyrimidine heterocyclic ring. Propoxazepam also has interaction with GLN 443 by halogen bond. All investigated benzodiazepines except 3-hydroxypropoxazepam create pi-pi stacking interaction with PHE 414 as NVW. Only propoxazepam has water-bridged hydrogen bonds with ASN 395 through the oxygen of the amide group (Fig. 1).

NVW is also involved in the interaction with ASN 395, but by the oxygen of thiopyrandioxyde.

6IM6: As determined by molecular docking (Schrödinger Maestro) Propoxasepam doesn't create a stable complex with 6IM6. Diazepam and oxazepam and AH3 establish pi-pi stacking interaction with PHE 372 (Q pocket).

2FM0: All investigated ligands form pi-pi stacking interaction with TYR 159 (Q pocket). Referring to Figure 2, propoxazepam and its metabolite 3-hydroxypropoxazepam occupied the P-clamp and interacted with the key residues ILE 336 and PHE 372.

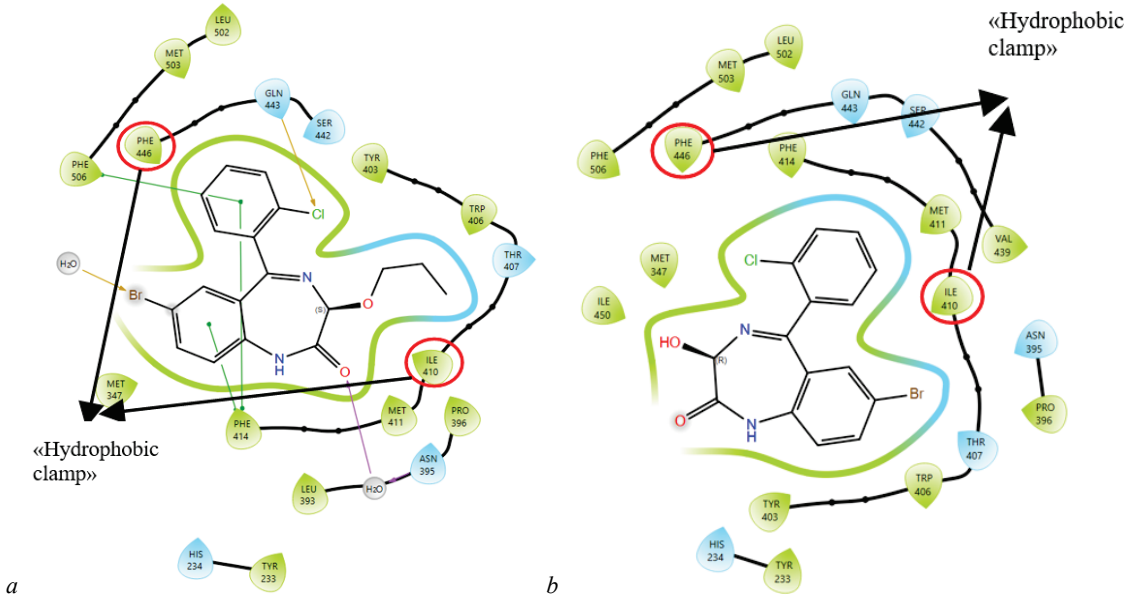

Fig. 1. Visualized position in specific binding sites PDE4B (3W5E) of the investigated ligands: propoxazepam (*a*), 3-hydroxypropoxazepam (*b*) (Schödinger Suite): LEU – leucine, MET – methionine, PHE – phenylalanine, GLN – glutamine, SER – serine, TYR – tyrosine, TRP – tryptophan, THR – threonine, ILE – isoleucine, PRO – proline, ASN – asparagine, MET – methionine, HIS – histidine, VAL – valine

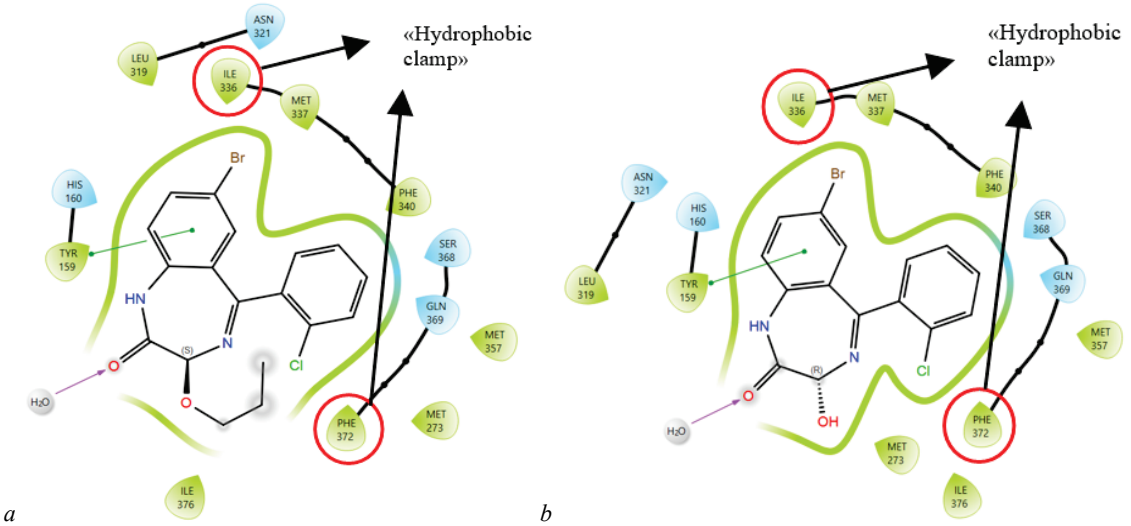

Fig. 2. Visualized position in specific binding sites PDE4D (2FM0) of the investigated ligands: propoxazepam (*a*), 3-hydroxypropoxazepam (*b*) (Schödinger Suite): see Figure 1

According to the results of the structural interaction fingerprints and the predicted values of the per-residue interaction score (Table 4–6) it is possible to analyse the common and different features of the contributions of amino acid residues of the active centre of phosphodiesterase with different ligands.

PDE4A: In the complex 3I8V with studied ligands PHE 584, PHE 552, ILE 548 amino acids residues have the biggest contribution in binding energy and are involved in the largest number of interactions with all investigated substances. 3-hydroxypropoxazepam has the largest number of ligand interactions among benzodiazepines. Compared to the reference ligand of 3I8V 0MO, propoxazepam has approximately the same amount of interaction with hydrophobic and polar residues. Mainly propoxazepam creates interaction with residues GLN 581 and ASN 533 by halogen atom Br. Residue ILE 548 (3TVX) creates the biggest amount of interaction with ligands and also has a high level of contributions in binding energy (-5.0 kcal/mol diazepam, -3.8 kcal/mol propoxazepam, -3.7 kcal/mol oxazepam, -1.6 kcal/mol 3-hydroxypropoxazepam and -4.6 kcal/mol reference ligand PNX) (Table 4).

PDE4B: GLN 443 (4KP6) forms interaction with all ligands: 3-hydroxypropoxazepam creates this interaction by Br atom, oxazepam through methyl group of benzene ring, propoxazepam has 2 interactions with this residue, by carbon atoms of chlorophenyl ring, diazepam forms this bond by oxygen of amide group and reference ligand 1S1 by nitrogen of triazole heterocycle, nitrogen of triazine heterocycle and carbon of methyl group. PHE 446, PHE 414 (4KP6) have the largest count of residue interactions and high value of per-residue interaction score: diazepam (-6.7, -1.8 kcal/mol), propoxazepam (-5.8, -3.4 kcal/mol), oxazepam (-5.1, -2.2 kcal/mol), 3-hydroxypropoxazepam (-4.7, -2.2 kcal/mol), reference ligand 1S1 (-8.6, -3.1 kcal/mol) (Table 5). Propoxazepam and 1S1 create interaction with TYR 233 by bromide atom (propoxazepam) and by

nitrogen of triazine heterocycle (1S1). The interactions were observed in the region surrounding TYR 233-ILE450 (3W5E) due to the presence of the active site in that region. GLN 443, PHE 446, PHE 414, ILE 410, ASN 395, MET 347 (3W5E) have significant contributions in the binding energy for all ligands (Table 5).

PDE4D: LEU 319, TRP 332, ILE 336, PHE 340, MET 357, SER 368, GLN 369, PHE 372 play a crucial role in the interaction of ligands in the binding site of 6IM6. In the complex 2FM0 with investigated ligands, residues TYR 159, MET 273, ASN 321, ILE 336, PHE 340, MET 357, GLN 369, PHE 372 have a great contribution in the binding energy. Among all ligands, only propoxazepam and reference ligand M98 create hydrophobic interaction with ILE 376.

Molecular dynamics. Molecular dynamics (MD) is essential since molecular docking studies of compound candidates' binding to target proteins may not be sufficient. The purpose of MD is to determine the stability of ligand–protein complexes using a system that simulates the conditions in the human body. The RMSD and RMSF values were used to determine stability and flexibility in this study. High deviations and protein fluctuations can be a sign of instability during simulations (Ongtanasup et al., 2022). RMSD was calculated for backbone atoms of PDE4A (3TVX), PDE4B (3W5E) and PDE4D (6IM6) complexes relative to the docked structures (AutoDock Vina) to assess dynamic stabilization over the time scale of the simulation period (Table 7).

Table 4
Per-residue interaction score of the studied complex of ligands and active center of PDE4A

Amino acid residues	Diazepam		Propoxazepam		Oxazepam		3-hydroxpropoxazepam		Reference ligand	
	3I8V	3TVX	3I8V	3TVX	3I8V	3TVX	3I8V	3TVX	3I8V	3TVX
PHE 584	–6.4	–5.3	–6.6	–5.9	–5.9	–4.5	–3.9	–0.6	–4.5	–5.8
TYR 371	–2.6	–3.3	–1.8	–1.9	–2.3	–4.3	–0.9	–0.9	–2.2	–4.1
ASN 533	–1.2	–2.4	–1.6	–5.3	–1.4	–2.9	0.3	0.0	–0.4	–1.1
GLN 581	–2.4	–3.1	–1.6	–1.8	–2.3	–1.8	–1.4	–0.3	–4.5	–3.1
MET 485	–2.7	–1.6	–4.9	–2.8	–2.3	–2.8	–5.9	–3.1	–2.5	–2.0
LEU 531	–1.2	–2.1	–0.9	–3.0	–1.3	–2.7	–1.9	–1.3	–1.3	–2.6
ILE 548	–5.6	–5.0	–4.9	–3.8	–5.4	–3.7	–2.9	–1.6	–3.8	–4.6
PHE 552	–3.2	–3.0	–4.3	–2.3	–3.5	–2.2	–2.9	–2.1	–1.9	–1.7

Notes: see Table 3, Figure 1.

Table 5
Per-residue interaction score of the studied complex of ligands and active center of PDE4B

Amino acid residues	Diazepam		Propoxazepam		Oxazepam		3-hydroxpropoxazepam		Referent ligand	
	4KP6	3W5E	4KP6	3W5E	4KP6	3W5E	4KP6	3W5E	4KP6	3W5E
GLN 443	–2.3	–2.3	0.1	–3.6	–1.4	–3.4	–1.5	–0.7	–4.7	–5.1
PHE 446	–6.7	–3.0	–5.8	–5.8	–5.1	–6.2	–4.7	–4.3	–8.6	–7.7
PHE 414	–1.8	–3.3	–3.4	–1.5	–2.2	–3.5	–2.2	–1.9	–3.1	–7.5
ASN 395	–0.8	–2.6	–0.5	–1.6	–0.5	–1.4	–0.4	–2.3	–3.7	3.6
ASP 392	–2.2	–1.8	–4.1	–3.2	1.5	–2.0	0.3	–0.2	–5.4	2.3
TYR 233	–2.1	–3.5	–1.7	–2.3	–1.6	–4.5	–1.1	–2.3	–2.3	–1.4
MET 431	–1.0	0	–1.7	0	–0.9	0	–1.1	0	–1.3	–0.4
ILE 410	–3.9	–4.6	–1.9	–4.3	–2.4	–4.2	–2.3	–3.8	–4.3	–5.6
MET 347	–2.6	–1.1	–2.7	–0.5	–4.4	–1.6	–4.5	–0.9	–2.2	–3.4

Notes: see Table 3, 4, Figure 1, ASP – aspartic acid.

Table 6
Per-residue interaction score of the studied complex of ligands and active center of PDE4D

Amino acid residues	Diazepam		Propoxazepam		Oxazepam		3-hydroxypropoxazepam		Referent ligand	
	6IM6	2FM0	6IM6	2FM0	6IM6	2FM0	6IM6	2FM0	6IM6	2FM0
HIP 160	–2.6	–1.9	–	–1.6	–4.0	–1.6	–1.3	–1.4	–7.2	–2.1
GLN 369	–3.6	–2.2	–	–1.5	–3.8	–1.4	–2.2	–1.2	–4.5	–5.5
TYR 159	–2.1	–1.7	–	3.1	–1.9	–3.0	0.9	–3.3	–2.2	–3.1
PHE 372	–4.1	–6.4	–	–6.9	–3.6	–5.7	–3.1	–7.2	–4.7	–6.4
PHE 340	–3.1	–3.1	–	–3.4	–2.9	–3.4	–1.6	–3.2	–2.4	–3.5
MET 273	–2.0	–2.1	–	–3.8	–1.2	–3.2	–1.6	–3.4	–1.0	–8.1
MET 357	0.9	–1.3	–	–2.4	0.9	–1.6	6.1	–1.6	–1.9	–3.5
SER 368	–1.5	–1.4	–	–1.5	–1.7	–1.4	–1.5	–1.4	–1.1	0
ASN 321	–1.9	–2.5	–	–1.1	–1.5	–0.6	–1.3	–0.8	–0.9	–1.7
LEU 319	–1.5	–1.3	–	–1.0	–1.6	–1.3	–1.4	–1.2	–0.8	–2.5
TYR 159	–2.1	–1.7	–	–3.1	–1.9	–3.0	0.9	–3.3	–2.2	–3.1
TRP 332	–0.6	–1.3	–	–0.9	–0.9	–0.7	–1.6	–0.7	–1.2	–0.7
ILE 336	–2.4	–5.1	–	–4.7	–2.3	–4.3	–0.4	–4.2	–4.4	–4.3

Notes: see Table 3, 4, Figure 1, HIP – histidine with hydrogens on both nitrogens.

According to the Figure 3b protein PDE4B (3W5E) in complex with 3-hydroxypropoxazepam has more fluctuation than propoxazepam or reference ligand at 9–10 ns.

The RMSF analysis was conducted to evaluate the mobility of the residues after binding to the ligands. We found one peak of fluctuations with high mobility in PDE4A (3TVX) (Fig. 4a). It is the residue MET 289 (in the plot -1), the RMSF for PDE4A without ligand is 5.82 Å, for complex PDE4A – PNX (reference ligand) – 4.49 Å, for complex PDE4A-3-hydroxypropoxazepam – 6.65 Å, and complex PDE4A – propoxazepam 3,76 Å. The residues ASP 230-VAL 231 (in the plot 77–78) have the biggest peak of fluctuations (Fig. 4b). HIS 234 (in the plot 81) – CYS 432 (in the plot 279) are region of PDE4B active site. Based on the results of MD demonstrated in the plot of Figure 4b) the M pocket of PDE4B (region HIS 234 (in the plot 81) – MET 347 (in the plot 194)) showed RMSF value in the range of 0.38–3.00 Å for protein without ligand, 0.46–1.95 Å for complex PDE4B-NVW, 0.44–2.65 Å complex PDE4B-3-hydroxypropoxazepam, 0.44–2.69 Å complex PDE4B – propoxazepam.

Referring to the plot in Figure 4c, there are three peaks (corresponding to three different protein regions) of fluctuations with high mobility in PDE4D (6IM6). The first one is placed on residues GLU 87 – GLU 89 (in the plot 1–3), the second and the highest one between residues SER 217 – GLU 218 (in the plot 131 to 132), the third involved the residue PRO 411 (in the plot 325).

Discussion

Activated G proteins are frequently associated with adenylyl cyclase, a membrane-associated enzyme that, when activated by the GTP-bound

alpha subunit, synthesizes cAMP from molecules of ATP. It is interesting to note that cAMP is only degraded enzymatically through hydrolysis by phosphodiesterase (PDE) enzymes. The pivotal role of PDE4 enzymes in cAMP signalling makes them interesting pharmacological targets for modulating cAMP levels in a variety of disorders. Therefore, PDE4 inhibition has been studied as a therapeutic approach to enhance cAMP signalling (Paes et al., 2022).

Scientific research has shown that the positive modulation of the stimulation of a cAMP response element reporter (CRE) through α1-AR activation was attributed to diazepam's ability to inhibit phosphodiesterase (PDEs), a known target of some benzodiazepines. Gαq/11G proteins signal α1-ARs, activating protein phospholipase C (PLC). PLC forms diacylglycerol (DAG), activating phosphokinase C (PKC) and inositol trisphosphate (IP3) for Ca^{2+} release. The stimulation of cAMP production through calmodulin-stimulated adenylate cyclase (AC) is also a secondary effect of AR activation. It is possible that PKC and secondary G protein coupling are also involved in AC activation (Fig. 5a) (Williams et al., 2019).

PDE4 inhibitors prevent pain by enhancing Cx43 expression through cAMP-PKA signalling in the spinal dorsal horn. Among PDEs, PDE4 is the primary one responsible for cAMP hydrolysis in nerve and immune cells. Inhibiting PDE4 has antinociceptive and anti-inflammatory effects in the brain. Additionally, PDE4 regulates the production of inflammatory cytokines by degrading cAMP (Fig. 5b) (Guo et al., 2016; Li et al., 2018; Al-Nema et al., 2020).

Table 7
The root mean square deviation (RMSD) of the protein (PDE4) in complex with researched ligands

3TVX	6 ns	12 ns	Range
Without ligand	0.945 Å	1.334 Å	0.389 Å
Reference ligand PNX	0.839 Å	1.273 Å	0.434 Å
Propoxazepam	0.837 Å	1.095 Å	0.258 Å
3-hydroxy-propxazepam	0.916 Å	1.244 Å	0.328 Å
3W5E	5 ns	10 ns	Range
Without ligand	1.015 Å	1.216 Å	0.201 Å
Reference ligand NVW	0.907 Å	1.293 Å	0.386 Å
Propoxazepam	0.815 Å	1.244 Å	0.429 Å
3-hydroxy-propxazepam	0.927 Å	1.875 Å	0.948 Å
6IM6	5 ns	10 ns	Range
Without ligand	0.868 Å	1.061 Å	0.193 Å
Reference ligand AH3	0.818 Å	1.205 Å	0.387 Å
Propoxazepam	0.836 Å	1.299 Å	0.463 Å
3-hydroxy-propxazepam	0.741 Å	1.276 Å	0.535 Å

Notes: see Table 3.

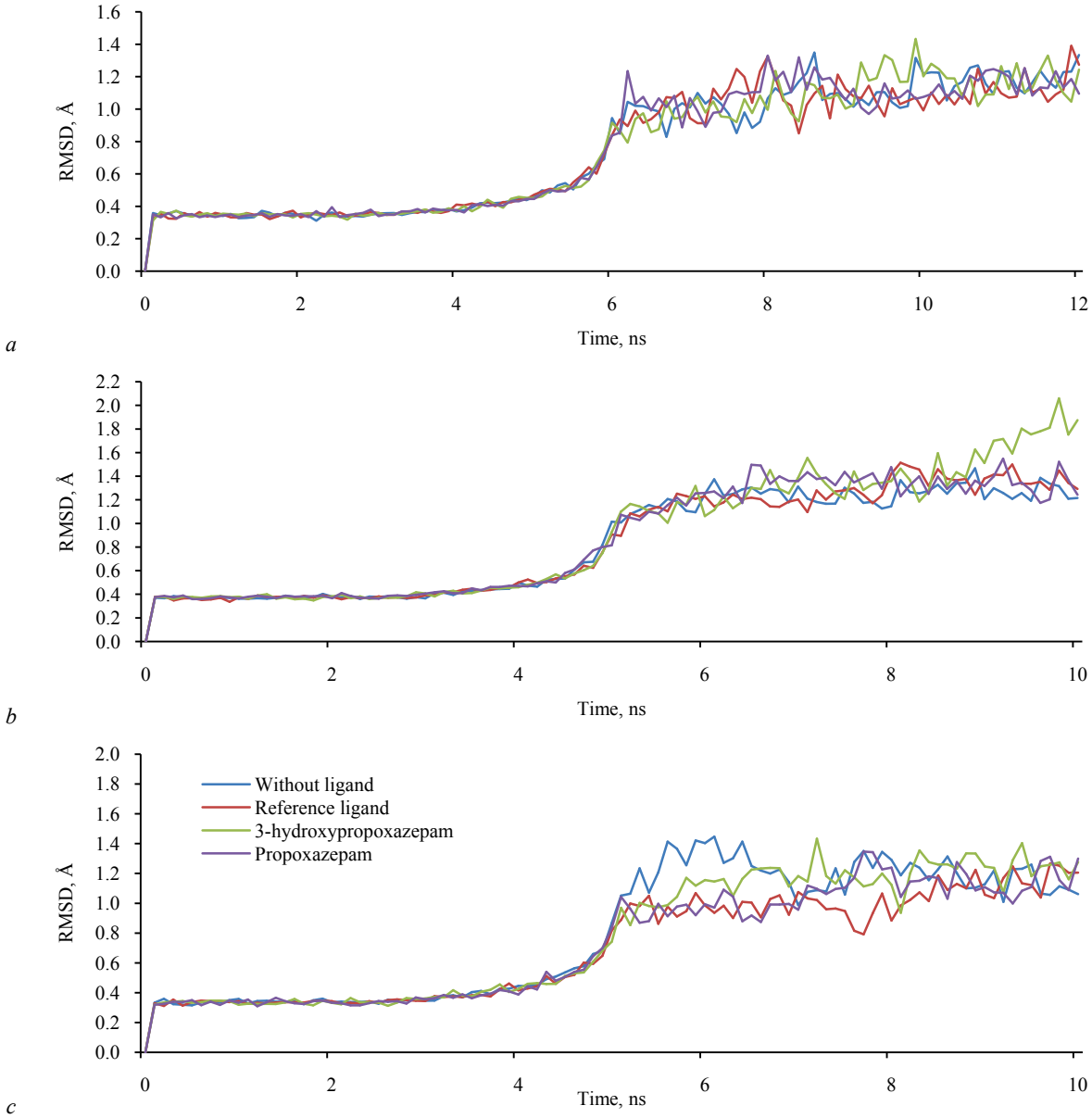

Fig. 3. RMSD values of PDE4 without and in complex with ligands: *a* – PDE4 (3TVX), reference ligand – PNX, *b* – PDE4B (3W5E), reference ligand – NVW, *c* – PDE4D (6IM6), reference ligand – AH3: RMSD – root mean square deviation

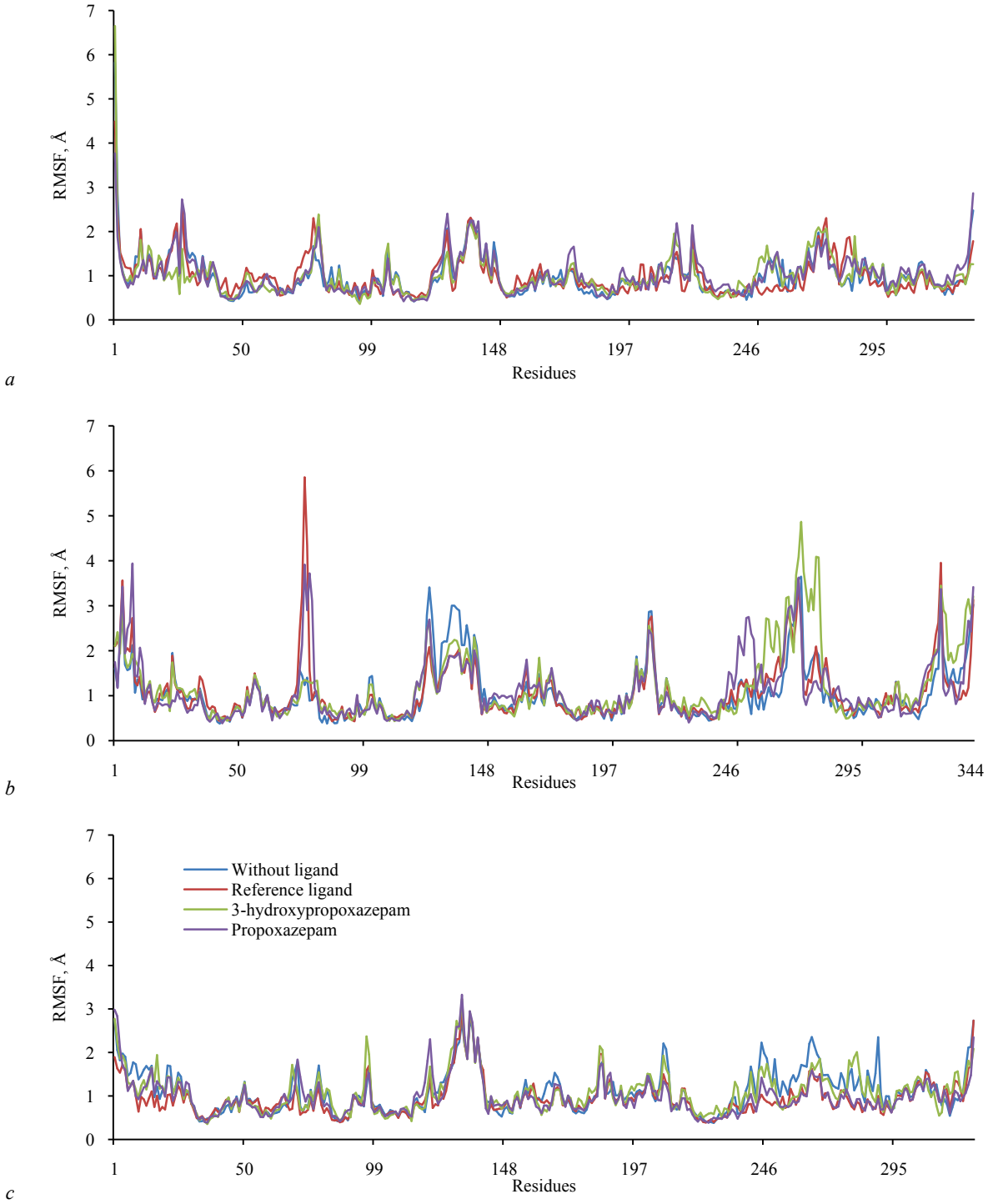

a

b

c

Fig. 4. RMSF values of PDE4 without and in complex with ligands: *a* – PDE4 (3TVX), reference ligand – PNX, *b* – PDE4B (3W5E), reference ligand – NVW, *c* – PDE4D (6IM6), reference ligand – AH3: RMSF – root mean square fluctuation

The structural characteristics of PDE4 were determined by reviewing the scientific literature to conduct a detailed analysis of the interaction mechanisms between benzodiazepines and PDE4. The structural features of PDEs are similar, with a conserved catalytic domain of ~300 amino acids located in the C-terminal part of the protein, and most PDE isoforms have regulatory regions that are specifically for families in their N-terminal portions (Bizzi et al., 2019). The active site is composed of three subpockets: M pocket (contains the metal ions (Zn^{+2} and Mg^{+2}), that are important for catalysis the hydrolysis of cAMP), Q pocket (is the most important domain for PDE4D inhibition and further divided into hydrophobic clamp (P-clamp) and conserved purine-selective glutamine), S pocket (signifies the solvent filled side pocket which has polar residues). The active site binds PDE inhibitors via a "hydrophobic clamp", a critical feature of hydrophobic interaction and common binding mode. This clamp, formed by a pair of highly conserved hydrophobic residues, typically includes phenylalanine (F4464B, F3724D) on one side in most PDE family members. The opposite side of the clamp is always hydrophobic, with varying compositions such as valine, leucine, or isoleucine (I4104B, I3364D) in different PDEs (Card et al., 2004).

After evaluating these studies, we performed docking on benzodiazepines and reference molecules with different Cryo-EM structures of α 1A-adrenergic receptors and with various PDE4 subtypes to examine the components of the interactions between these ligands and proteins.

α1A adrenergic receptor. Oxymetazoline has the lowest Ki value (16 nM) among the three reference compounds, indicating the highest binding affinity to the target. Its ΔGexp (-12.07 kcal/mol) and MMGBSA

(-83.89 kcal/mol) values are also notably more negative than those of norepinephrine and epinephrine, further suggesting strong binding (Table 2). The MMGBSA values for the reference compounds (Norepinephrine and Epinephrine, Oxymetazoline) corresponded well with their experimental values, it strengthens the reliability of the MMGBSA method for predicting binding affinities of the investigated ligands to the protein. 3-hydroxypropoxazepam, compared to propoxazepam shows better predicted affinity values for the alpha 1A adrenergic receptor, creating more hydrogen bonds by hydroxyl group.

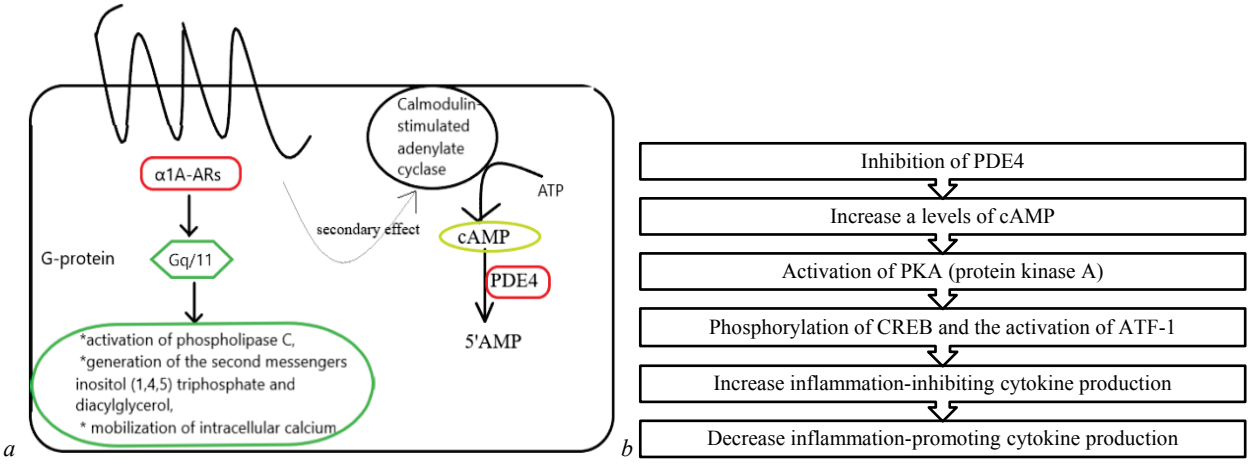

Fig. 5. Cascade of process modulated of a cAMP response element pathway by α1A-ARs by off-target inhibition of phosphodiesterase (*a*); cascade of antinociceptive and anti-inflammatory process of PDE4 (*b*): α1A-ARs – alpha-1A adrenergic receptors, Gαq/11 – type of G protein, cAMP – cyclic adenosine monophosphate, PDE4 – phosphodiesterase 4, 5'-AMP – 5'-adenosine monophosphate, PKA – protein kinase A, CREB – cAMP response element-binding protein, ATF-1 – activating transcription factor 1

Phosphodiesterase 4. Propoxazepam generally exhibits stronger binding affinities compared to diazepam and oxazepam across various PDE4 isoforms as evident from the more negative predicted binding energies across all computational methods. This suggests that propoxazepam may have a higher potential for binding to PDE4 isoforms. Its metabolite 3-hydroxypropoxazepam shows slightly lower binding energies than propoxazepam in some cases, these values still indicate significant binding affinity (Table 3).

PDE4A: Propoxazepam and its metabolite 3-hydroxypropoxazepam exhibit favourable interactions with PDE4A, as indicated by low MMGBSA values and strong binding energies calculated by Vina (Table 3). Certain residues, such as PHE 584, ILE 548 and TYR 371, consistently exhibit strong interactions with multiple ligands across both protein structures, mostly by pi-pi stacking interaction (3I8V, 3TVX) (Table 4). This suggests their importance in ligand recognition and binding. MD simulations were performed for 12 ns using the docked conformation of PDE4A 3TVX – ligand complexes to investigate the atomic details of molecular interactions. As specified by Table 7, the initial RMSDs after the first 6 ns and the final RMSDs for 3TVX in complex with reference ligands (PNX) as a positive control were 0.839 Å and 1.273 nm, respectively, over the entire simulation period (fluctuation: 0.434 Å). Thus, good chemical candidates should have an RMSD range of less than 0.434 Å. During the simulation period, the initial RMSD after the first 6 ns and the final RMSDs for the 3TVX protein-propoxazepam complex were 0.837 and 1.095 Å, respectively (fluctuation: 0.258 Å). The RMSD values of PDE4A(3TVX) in complex with propoxazepam were smaller than that of the PDE4A without ligand and PDE4A with reference ligand (PNX). It indicates that propoxazepam can stabilize the protein. PDE4A in complex with 3-hydroxypropoxazepam have also fewer fluctuations than a positive control also in complex with PDE4A(3TVX) (Fig. 3a). All RMSD values were below 2 Å, indicating stable ligand poses for all MD simulations. Propoxazepam attachment to PDE4A reduces fluctuations in this residue MET 289 (in the plot 1). The mobility of residues in PDE4A complexes is lower than that of residues in PDE4B and PDE4D complexes, which may indicate a higher stability of the protein-ligand complex (Fig. 4).

PDE4B: According to AutoDock Vina and MMGBSA predicted results, 3-hydroxypropoxazepam create the most stable complex among other benzodiazepines with PDE4B(4KP6), having the lowest values of free binding energy -9.8 and -29.1 kcal/mol, respectively. Propoxazepam exhibits strong binding affinities (-10.3 kcal/mol) with PDE4B (3W5E) compared to diazepam (-9.3 kcal/mol) and 3-hydroxypropoxazepam (-9.3 kcal/mol) as evident from the more negative predicted binding energies across AutoDock Vina (Table 3). Propoxazepam and its metabolite 3-hydroxypropoxazepam are located in the active site of PDE4B (3W5E) and create interactions with residues of Q pocket, in the hydrophobic clamp (P-clamp) PHE 446 and ILE 410, which is a crucial feature of hydrophobic interaction of inhibitors with PDE4B (Fig. 1) (Coghi et al., 2021). Residues TYR 233, GLN 443, ILE 410 and PHE 446 (Q pocket) and PHE 414 (S pocket) have the highest pre-residue interaction scores, which means a crucial role of these residues in the interaction (Table 5). RMSD value of PDE4B(3W5E)-propoxazepm complex is slightly higher (0.429 Å) than RMSD for protein without ligand (0.201 Å) or with reference ligand – NVW (0.386 Å) (Table 7). This could indicate differences in binding specificity or affinity between propoxazepam and the protein compared to the reference ligand. RMSF results of PDE4B indicate lower fluctuations of the residues of M pocket (the most conserved among PDE4 enzyme structure) of the catalytic domain in the complex protein – ligand (all investigated compounds) compared to protein without ligand and supporting the docking findings that binding of the ligand stabilizes the protein structure (Fig. 4).

PDE4D: AutoDock Vina prediction results revealed that propoxazepam and 3-hydroxypropoxazepam have the lowest docking scores (-8.8 and -9.0 kcal/mol), which signify high affinity of these ligands to 6IM6. In contrast to Vina, Schrodinger Suite demonstrates creation of unstable complex 6IM6-propoxazepam (Table 3). But its metabolite 3-hydroxypropoxazepam forms the similar hydrogen bond with HIP 160 (6IM6) (M pocket) by oxygen of amide group as reference ligand AH3 (by oxygen of aldehyde group), which emphasizes the similarity of interaction mechanisms. Propoxazepam has the highest predicted free binding energy with 2FMO according to the MMGBSA method (-52.6 kcal/mol), followed by 3-hydroxypropoxazepam (-43.9 kcal/mol) (Table 3). Residues PHE 372 and ILE 336 have one of the highest contributions in the free binding energy for most ligands, especially for propoxazepam and its metabolite 3-hydroxyproxazepam (Table 6, Fig. 2). These residues play a significant role of hydrophobic interaction PDE inhibitors. RMSD range of PDE4D(6IM6) in complex with propoxazepam is higher than PDE4D(6IM6)-reference ligand complex, it means that complex with 1,4-benzodiazepine is less stable. Complexes 6IM6 – Propoxazepam and 6IM6-3-hydroxypropoxazepam have fewer fluctuations on the residues PHE 372 (in the plot 286), ILE 336 (in the plot 250) compared to protein without ligand (Fig. 4c). By stabilizing these residues, benzodiazepines create a stable hydrophobic interaction with it. It can be observed that the RMSD curves for the backbone atoms of the PDE4D (6IM6) skeleton

without a ligand reach 1.447 Å at 6.1 ns. But PDE4D (6IM6) in complex with propoxazepam RMSD is 0.971 Å (Fig. 3c). Therefore, the binding of propoxazepam made the complex more stable. The mobility of the residues of the PDE4D(6IM6) – 3-hydroxypropoxazepam complex and PDE4D without ligand was the highest among PDE4D complexes with ligands (Fig. 4c).

Conclusion

Propoxazepam has average MMGBSA predicted free binding energy (-38.5, -17.2, -6.9 kcal/mol) and Glide Score (-6.8, -6.2, -6.0 kcal/mol) in docking process with α1A-adrenoceptors (7YM8, 7YMH, 8THL), which indicates a moderate affinity of propoxazepam to α1A-AR. Its metabolite, 3-hydroxypropoxazepam shows better predicted affinity values for the α1-AR. Based on AutoDock Vina results, propoxazepam tends to exhibit moderate to strong binding affinities across various PDE4 types compared to reference ligands, with values ranging from -8.7 to -10.3 kcal/mol. The best predicted binding affinity is observed for PDE4B (3W5E) with a score of -10.3 kcal/mol.. According to Schödinger Suite prediction for PDE4 subtypes, propoxazepam demonstrates competitive or superior binding affinities compared to other ligands in most cases. Propoxazepam has the lowest MMGBSA value among other ligands with PDE4A (3I8V) -55.1 kcal/mol, PDE4D (2FMO) -52.6 kcal/mol, indicating strong interactions. Propoxazepam mainly forms the same hydrophobic interac. tions and pi-pi stacking interactions as reference ligands. Propoxazepam creates hydrogen bonds only with PDE4A (3TVX) ASP 530 through the amide group and with ASN 533 by oxygen of alkoxy group. Propoxazepam and its metabolite 3-hydroxypropoxazepam interact with active sites of PDE4B (3W5E) and PDE4D (2FMO) with the help of a "hydrophobic clamp", which is a crucial feature of hydrophobic interaction and the common binding mode for PDE inhibitors. The RMSD values for the PDE4A(3TVX) complex with propoxazepam were observed to be smaller than those of the positive control, suggesting the formation of stable protein-propoxazepam complex, implying potential effectiveness and reliability of propoxazepam as a PDE4A inhibitor. The range of RMSD values for PDE4B (3W5E) and PDE4D (6IM6) in complexes with 1,4-benzodiazepines are higher than complexes of these proteins with reference ligands or without ligands. It is possible that there are differences in the binding specificity or affinity between propoxazepam and the protein compared to the reference ligand. The obtained results make it possible to predict the binding mechanisms of 1,4-benzodiazepines with the alpha 1A adrenoceptor and phosphodiesterase 4 and reflect the similarity in the molecular interaction of 1,4-benzodiazepines with phosphodiesterase 4 inhibitors, which allows one to theoretically predict the inhibitory effect of propoxazepam and its possible metabolite 3-hydroxopropoxazepam on phosphodiesterase 4. Further research in these areas may provide valuable insight into the therapeutic potential of propoxazepam and its metabolite as PDE4 inhibitors and guide the development of new analgesics and anti-inflammatory drugs for diseases where α 1A-adrenergic receptor and PDE4 regulation plays a role.

The authors express their gratitude to SLC "Interchem" and O. V. Bogatsky Physico-Chemical Institute of the National Academy of Sciences of Ukraine for providing consultation about investigated substance "Propoxazepam" and its metabolite 3-hydroxypropoxazepam.

The authors have no conflicts of interest relevant to the content of this article.

References

Agu, P. C., Afiukwa, C. A., Orji, O. U., Ezeh, E. M., Ofoke, I. H., Ogbu, C. O., Ugwuja, E. I., & Aja, P. M. (2023). Molecular docking as a tool for the discovery of molecular targets of nutraceuticals in diseases management. Scientific Reports, 13, 13398.

Al-Nema, M., Gaurav, A., & Lee, V. S. (2020). Docking based screening and molecular dynamics simulations to identify potential selective PDE4B inhibitor. Heliyon, 6(9), E04856.

Azevedo, M. F., Faucz, F. R., Bimpaki, E., Horvath, A., Levy, I., de Alexandre, R. B., Ahmad, F., Manganiello, V., & Stratakis, C. A. (2014). Clinical and molecular genetics of the phosphodiesterases (PDEs). Endocrine Reviews, 35(2), 195–233.

Baillie, G. S., Tejeda, G. S., & Kelly, M. P. (2019). Therapeutic targeting of 3′,5′-cyclic nucleotide phosphodiesterases: Inhibition and beyond. Nature Reviews Drug Discovery, 18, 770–796.

Barakat, A., Munro, G., & Heegaard, A. M. (2024). Finding new analgesics: Computational pharmacology faces drug discovery challenges. Biochemical Pharmacology, 222, 116091.

Beihong, J., Shuhan, L., Xibing, H., Viet, H. M., Xiang-Qun, X., & Junmei, W. (2020). Prediction of the binding affinities and selectivity for CB1 and CB2 ligands using homology modeling, molecular docking, molecular dynamics simulations, and MM-PBSA binding free energy calculations. ACS Chemical Neuroscience, 11(8), 1139–1158.

Bizzi, M. F., Bolger, G. B., Korbonits, M., & Ribeiro-Oliveira Jr., A. (2019). Phosphodiesterases and cAMP Pathway in Pituitary Diseases. Frontiers in Endocrinology, 10, 141.

Card, G. L., England, B. P., Suzuki, Y., Fong, D., Powell, B., Lee, B., Luu, C., Tabrizizad, M., Gillette, S., Ibrahim, P. N., Artis, D. R., Bollag, G., Milburn, M. V., Kim, S. H., Schlessinger, J., & Zhang, K. Y. (2004). Structural basis for the activity of drugs that inhibit phosphodiesterases. Structure, 12(12), 2233–2247.

Chu, Z., Xu, Q., Zhu, Q., Ma, X., Mo, J., Lin, G., Zhao, Y., Gu, Y., Bian, L., Shao, L., Guo, J., Ye, W., Li, J., He, G., & Xu, Y. (2021). Design, synthesis and biological evaluation of novel benzoxaborole derivatives as potent PDE4 inhibitors for topical treatment of atopic dermatitis. European Journal of Medicinal Chemistry, 213, 113171.

Coghi, P., Yang, L. J., Ng, J. P. L., Haynes, R. K., Memo, M., Gianoncelli, A., Wong, V. K. W., & Ribaudo, G. (2021). A drug repurposing approach for antimalarials interfering with SARS-CoV-2 spike protein receptor binding domain (RBD) and human angiotensin-converting enzyme 2 (ACE2). Pharmaceuticals, 14(10), 954.

Friesner, R. A., Murphy, R. B., Repasky, M. P., Frye, L. L., Greenwood, J. R., Halgren, T. A., Sanschagrin, P. C., & Mainz, D. T. (2006). Extra precision glide: Docking and scoring incorporating a model of hydrophobic enclosure for protein-ligand complexes. Journal of Medicinal Chemistry, 49(21), 6177–6196.

Ghode, P., & Jain, S. K. (2018). Structural requirements for some 3-amino-N-substituted-4-(substituted phenyl) butanamides as dipeptidyl peptidase-IV inhibitors using 3D-QSAR and molecular docking approaches. Indian Journal of Pharmaceutical Sciences, 79(6), 974–986.

Gianoncelli, A., Ongaro, A., Zagotto, G., Memo, M., & Ribaudo, G. (2020). 2-(3,4-Dihydroxyphenyl)-4-(2-(4-nitrophenyl)hydrazono)-4H-chromene-3,5,7-triol. Molbank, 3, M1144.

Golovenko, M. Y. (2021). Propoksazepam – novatorskyi analhetychnyi zasib, shcho halmuie hostryi ta khronichnyi bil i maie polimodalnyi mekhanizm dii [Propoxazepam – an innovative analgesic that inhibits acute and chronic pain and has a polymodal mechanism of action]. Visnyk NAN Ukrainy, 4, 76–90 (in Ukrainian).

Golovenko, M., Reder, A., Zupanets, I., Bezugla, N., Larionov, V., & Valivodz, I. (2023). A phase I study evaluating the pharmacokinetic profile of a novel oral analgesic propoxazepam. Journal of Pre-Clinical and Clinical Research, 17(3), 138–144.

Golovenko, N. Y., Voloshchuk, N. I., Andronati, S. A., Taran, I. V., Reder, A. S., Pashynska, O. S., & Larionov, V. B. (2018). Antinociception induced by a novel benzodiazepine receptor agonist and bradykinin receptor antagonist in rodent acute and chronic pain models. European Journal of Biomedical and Pharmaceutical Sciences, 5(12), 79–88.

Guo, C.-H., Bai, L., Wu, H.-H., Yang, J., Cai, G.-H., Wang, X., Wu, S.-X., & Ma, W. (2016). The analgesic effect of rolipram is associated with the inhibition of the activation of the spinal astrocytic JNK/CCL2 pathway in bone cancer pain. International Journal of Molecular Medicine, 38(5), 1433–1442.

Halgren, T. A. (2009). Identifying and characterizing binding sites and assessing druggability. Journal of Chemical Information and Modeling, 49(2), 377–389.

Jin, J., Mazzacuva, F., Crocetti, L., Giovannoni, M. P., & Cilibrizzi, A. (2023). PDE4 inhibitors: Profiling hits through the multitude of structural classes. International Journal of Molecular Sciences, 24(14), 11518.

Kachkovska, V., Kovchun, A., Dudchenko, I., & Prystupa, L. (2023). GLN27GLU polymorphism in the β2 adrenoreceptor gene in patients with asthma with regard to the age of onset. Eastern Ukrainian Medical Journal, 11(4), 390–397.

Li, H., Zuo, J., & Tang, W. (2018). Phosphodiesterase-4 inhibitors for the treatment of inflammatory diseases. Frontiers in Pharmacology, 9, 1048.

Martínez-Rosell, G., Giorgino, T., & De Fabritiis, G. (2017). Play molecule proteinprepare: A web application for protein preparation for molecular dynamics simulations. Journal of Chemical Information and Modeling, 57(7), 1511–1516.

Milligan, A. L., Szabo-Pardi, T. A., & Burton, M. D. (2020). Cannabinoid receptor type 1 and its role as an analgesic: An opioid alternative? Journal of Dual Diagnosis, 16(1), 106–119.

Mortier, J., Rakers, C., Bermudez, M., Murgueitio, M. S., Riniker, S., & Wolber, G. (2015). The impact of molecular dynamics on drug design: Applications for the characterization of ligand-macromolecule complexes. Drug Discovery Today, 20(6), 686–702.

Ongtanasup, T., Wanmasae, S., Srisang, S., Manaspon, C., Net-anong, S., & Eawsakul, K. (2022). *In silico* investigation of ACE2 and the main protease of SARS-CoV-2 with phytochemicals from *Myristica fragrans* (Houtt.) for the discovery of a novel COVID-19 drug. Saudi Pharmaceutical Journal, 29(9), 103389.

Paes, D., Hermans, S., Hove, D. van den, Vanmierlo, T., Prickaerts, J., & Carlier, A. (2022). Computational investigation of the dynamic control of cAMP signaling by PDE4 isoform types. Biophysical Journal, 121(14), 2693–2711.

Perez, D. M. (2020). A1-adrenergic receptors in neurotransmission, synaptic plasticity, and cognition. Frontiers in Pharmacology, 11, 581098.

Potluri, H., Prasanth, D. S., & Atmakuri, L. R. (2021). *In vivo* antinociceptive effect of methanolic extract of *Ipomoea marginate* Desr. in rodents as well as *in silico* molecular docking of some phytoconstituents from the plant. Indian Journal of Pharmaceutical Sciences, 83(4), 732–741.

Trott, O., & Olson, A. J. (2010). AutoDock Vina: Improving the speed and accuracy of docking with a new scoring function, efficient optimization and multithreading. Journal of Computational Chemistry, 31(2), 455–461.

Tsyndrenko, N., & Romaniuk, A. (2024). PVUII (RS2234693) polymorphism of the estrogen receptor alpha gene in women from Sumy oblast, Ukraine, with endometrial hyperplastic process. Eastern Ukrainian Medical Journal, 12(1), 160–173.

Williams, L. M., He, X., Vaid, T. M., Abdul-Ridha, A., Whitehead, A. R., Gooley, P. R., Bathgate, R. A. D., Williams, S. J., & Scott, D. J. (2018). Diazepam is not a direct allosteric modulator of α1-adrenoceptors, but modulates receptor signaling by inhibiting phosphodiesterase-4. Pharmacology Research and Perspectives, 7(1), e00455.

Xu, J., Yang, G., Li, T., & Liu, L. (2017). Myoendothelial gap junctions mediate regulation of angiopoietin-2-induced vascular hyporeactivity after hypoxia through connexin 43-gated cAMP transfer. American Journal of Physiology. Cell Physiology, 313(3), 262–273.

Yang, Y., Yao, K., Repasky, M. P., Leswing, K., Abel, R., Shoichet, B. K., & Jerome, S. V. (2021). Efficient exploration of chemical space with docking and deep learning. Journal of Chemical Theory and Computation, 17(11), 7106–7119.

Zhang, F., Wang, H., Zhou, Y., Yu, H., Zhang, M., Du, X., Wang, D., Zhang, F., Xu, Y., Zhang, J., & Zhang, H.-T. (2022). Inhibition of phosphodiesterase-4 in the spinal dorsal horn ameliorates neuropathic pain via cAMP-cytokine-Cx43 signaling in mice. CNS Neuroscience and Therapeutics, 28(5), 749–760.